International Journal of Pharmaceutics 396 (2010) 239–245

Contents lists available at ScienceDirect

International Journal of Pharmaceutics

journal homepage: www.elsevier.com/locate/ijpharm

Pharmaceutical Nanotechnology

Preparation and pharmaceutical characterization of amorphous cefdinir using spray-drying and SAS-process

Junsung Park, Hee Jun Park, Wonkyung Cho, Kwang-Ho Cha, Young-Shin Kang, Sung-Joo Hwang*

Center for Nanotechnology-based New Drug Dosage Form, College of Pharmacy, Chungnam National University, 220 Gung-dong, Yuseung-gu, Daejeon 305-764, Republic of Korea

ARTICLE INFO

Article history:
Received 12 April 2010
Received in revised form 1 June 2010
Accepted 18 June 2010
Available online 25 June 2010

Keywords:
Cefdinir
Amorphous
Anhydrous
Micronization
Supercritical anti-solvent (SAS)

ABSTRACT

The aim of this study was to investigate the effects of micronization and amorphorization of cefdinir on solubility and dissolution rate. The amorphous samples were prepared by spray-drying (SD) and supercritical anti-solvent (SAS) process, respectively and their amorphous natures were confirmed by DSC, PXRD and FT-IR. Thermal gravimetric analysis was performed by TGA. SEM was used to investigate the morphology of particles and the processed particle had a spherical shape, while the unprocessed crystalline particle had a needle-like shape. The mean particle size and specific surface area were measured by dynamic light scattering (DLS) and BET, respectively. The DLS result showed that the SAS-processed particle was the smallest, followed by SD and the unprocessed cefdinir. The BET result was the same as DLS result in that the SAS-processed particle had the largest surface area. Therefore, the processed cefdinir, especially the SAS-processed particle, appeared to have enhanced apparent solubility, improved intrinsic dissolution rate and better drug release when compared with SD-processed and unprocessed crystalline cefdinir due not only to its amorphous nature, but also its reduced particle size. Conclusions were that the solubility and dissolution rate of crystalline cefdinir could be improved by physically modifying the particles using SD and SAS-process. Furthermore, SAS-process was a powerful methodology for improving the solubility and dissolution rate of cefdinir.

1. Introduction

About 32% of the drugs on the market and more than 40% of recent candidates for new drugs are considered "poorly water soluble". For orally administered poorly water soluble compounds, in particular, the dissolution in gastro intestinal fluid is a critical factor for the bio-absorption process. Many processes, such as; salt formation (Engel et al., 2000; Han and Choi, 2007), solid dispersion (Chiou and Reigelman, 1971; Ford and Elliott, 1985; Kim et al., 2006), inclusion complex (Peeters et al., 2002; Al-Marzouqi et al., 2006; Jun et al., 2007) and microemulsion (Park et al., 2007) have been developed and well studied to improve the dissolution rate of poorly water soluble drugs. In addition, techniques improving physical modifications, such as micronization (Perrut et al., 2005; Kim et al., 2007), and generation of amorphous states (Hancock and Zografi, 1997; Kim et al., 2008b) techniques have been developed.

Micronization is a well known procedure used in the pharmaceutical industry to reduce the particle size of active pharmaceutical ingredients (API). This size reduction leads to an increase in specific surface area and consequently faster dissolution for API particles. Thus, if the dissolution rate was the limiting factor for bioavailability, increased bioavailability would be expected.

According to Linpinski et al. (1997), solubility of solid solute can be predicted by the crystal packing energy, which accounts for the energy necessary to disrupt the crystal packing and to bring isolated molecules in gas phases, i.e. its enthalpy of sublimation. A crystalline solid has relatively higher crystal packing energy than an amorphous solid, which means the amorphous solid has low packing energy and no long-range order of molecular packing. Therefore, an amorphous solid often has higher solubility than a crystalline solid, resulting in enhanced dissolution and bioavailability (Hancock and Parks, 2000; Dhumal et al., 2008; Kim et al., 2008a,b).

Cefdinir (8-[2-(2-amino-1,3-thiazol-4-yl)-1-hydroxy-2-nitroso-ethenyl]amino-4-ethenyl-7-oxo-2-thia-6-azabicyclo [4.2.0]oct-4-ene-5-carboxylic acid; Fig. 1) is a semi-synthetic third-generation broad-spectrum oral cephalosporin active against both Gram positive and negative bacteria (Budavari, 1996). Even though, it is used widely to treat acute chronic bronchitis, rhinosinusitis and pharyngitis, it has only 21–25% of oral bioavailability (Perry and Lesley, 2004), which is probably due to low aqueous solubility.

The objective of the present work was to study the effects of amorphorization and micronization on cefdinir. The amorphous form of cefdinir can be easily made by dissolving cefdinir into

* Corresponding author. Tel.: +82 42 821 5922; fax: +82 42 823 3078.
E-mail address: sjhwang@cnu.ac.kr (S.-J. Hwang).

0378-5173/$ – see front matter © 2010 Elsevier B.V. All rights reserved.
doi:10.1016/j.ijpharm.2010.06.032

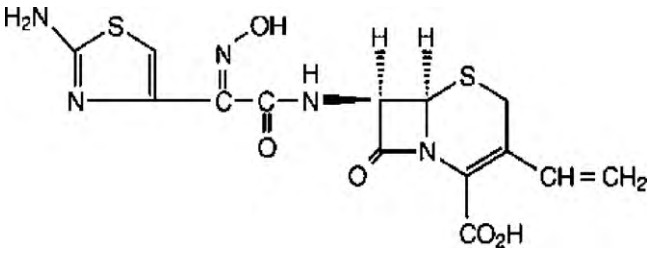

Fig. 1. Structure of cefdinir.

methanol and evaporating the solvent to obtain the powder. To compare the size effect, amorphous cefdinir was prepared by spray-drying (SD) and supercritical anti-solvent (SAS) process. Their phamaceutical properties were evaluated by DSC, TGA, PXRD, FT-IR, BET, SEM, solubility, intrinsic dissolution and tablet dissolution studies.

2. Material and methods

2.1. Materials

Cefdinir was obtained from Shinpoong Pharm Co., Ltd. (South Korea). Carbon dioxide (CO_2) with high purity of 99.9% was supplied from Hanmi Gas Co., Ltd. (South Korea). All organic solvents were high performance liquid chromatography (HPLC) grade. D-Mannitol and magnesium stearate were purchased from Samchun Chemical Co., Ltd. (South Korea) and PVP K30 was kindly obtained from BASF Co., Ltd. (Germany). All other chemicals were reagent grade.

2.2. Supercritical anti-solvent (SAS) process

The SAS-process was performed using the experimental equipment as previously described (Kim et al., 2008b). Cefdinir was dissolved in methanol. Then, the supercritical carbon dioxide (SC-CO_2) was pumped into the top of the particle precipitation vessel (approximately 1.9 l) through the outer capillary of the two-flow spray nozzle (drug solution was sprayed into the vessel via the central capillary tube and a secondary co-axical pathway surrounding the central capillary tube for passage of the SC-CO_2) at a constant rate using a Suflux pump (Model No.KMB01HK1F, Ilshin Autoclave Co. Ltd., Korea) until the desired pressure was obtained. The experiment was performed under the following conditions: temperature of particle precipitation vessel, 45 °C; pressure, 12 MPa; drug solution concentration, 20 mg/ml; feed rate, 2 ml/min; CO_2 flow rate, 45 g/min. The drug solution was introduced into the particle precipitation vessel by a HPLC liquid pump (Model 307, Gilson Inc., USA) through the two-flow spray nozzle. Meanwhile, the SC-CO_2 continued to flow through the vessel to maintain the steady pressure. The residual solvent (SC-CO_2 and methanol) was drained out of the particle precipitation vessel by the backpressure regulator (model 26-1723-24-194, Tescom, UK). After spraying the drug solution into the particle precipitation vessel was completed, additional SC-CO_2 was continuously pumped into the vessel at the same rate for another 120 min to remove residual methanol content dissolved in the SC-CO_2. The precipitation vessel was slowly depressurized to atmospheric pressure. The precipitated particles were collected from the wall and bottom (retained by a 0.1 μm metal sieve and paper filter) of the particle precipitation vessel and then stored in a refrigerator.

2.3. Spray-drying (SD) process

Cefdinir was dissolved in methanol to obtain clear solutions. Spray-drying was performed using a laboratory scale spray dryer (SD 1000, Eyela, Japan) under the following set of conditions: drug solution concentration, 20 mg/ml; inlet temperature, 90 °C; outlet temperature, 45–50 °C; feed rate, 2 ml/min; atomization air pressure, 110 kPa; drying air flow rate, 0.70 m^3/min.

2.4. Scanning electron microscopy (SEM)

The morphology of particles was examined by scanning electron microscopy (SEM; JSM-7000F, Jeol Ltd., Japan).

2.5. Particle size analysis

The mean particle size of samples was determined by dynamic light scattering (DLS) using electrophoretic light scattering spectrophotometer (ELS-8000, Otsuka Eletronics, Japan). The samples were dispersed in mineral oil and sonicated for 10 min at 120 W (Branson 8210, Branson Ul-trasonics Co., USA). Information about the particle size was obtained by using the cumulant method to analyze the DLS data.

2.6. BET

The specific surface area of samples was determined by N_2 adsorption using the Surface Area Analyzer. ASAP 2010 (Micromeritics Instrument Corporation, USA).

2.7. Differencial scanning calorimetry (DSC)

DSC measurements were carried out by DSC S-650 (Scinco Co. Ltd., Korea). The samples of 3–4 mg were accurately weighed and sealed in aluminum pans. The measurements were performed over the range of 25–250 °C at a heating rate of 10 °C/min. An empty pan was used for the reference and indium was used to calibrate baseline, temperature, and enthalpy at a heating rate of 10 °C/min. A N_2 flow rate of 40 ml/min was used to purge each DSC run.

2.8. Thermal gravimetric analysis (TGA)

TGA was performed via a thermogravimetrical analyzer SDTQ600 (TA Instruments, USA) over a temperature range of 10–300 °C at a heating rate of 5 °C/min under a N_2 flow (50 ml/min) Approximately 5 mg of sample was placed in open aluminum pans and the weight loss was monitored.

2.9. Powder X-ray diffraction (PXRD)

PXRD patterns were recorded on a Rigaku Powder X-ray diffraction system (Model D/MAX-2200 Ultima/PC, Japan) with Ni-filtered Cu-Kα radiation. The samples were test over the most informative range from 5° to 70° of 2θ. The step scan mode was performed with a step size of 0.02° at a rate of 2°/min.

2.10. Fourier transform infrared (FT-IR) spectroscopy

FT-IR spectra were obtained on a FT-IR spectrometer (Thermo Fisher, Nicolet 380 FT-IR, USA) using an attenuated total reflectance (ATR) method. The scanning range was 650–4000 cm^{-1} and the resolution was 4 cm^{-1}. The number of reference scans was 64.

2.11. Solubility studies

Saturation solubility of cefdinir was determined in distilled water at 25 ± 0.5 °C. The samples were placed in a shaking water bath (60 rpm) for 24 h previously determined to be adequate time for equilibration. Suitable aliquots were withdrawn in certain time intervals and filtered using a 0.2 μm nylon syringe filter. The filtrate

was diluted with mobile phase, and the concentration of cefdinir was determined by HPLC. In addition, for kinetic solubility studies, excess solid (approximately 1 g of cefdinir) was placed in 200 ml water in a water-jacketed vessel linked to a temperature controlled water bath held at 25 ± 0.5 °C. Solutions were agitated constantly by overhead stirrers at 200 rpm. Suitable aliquots were withdrawn in certain time intervals and filtered using a 0.2 μm nylon syringe filter. The filtrate was diluted with mobile phase, and the concentration of cefdinir was determined by HPLC. Chromatographic analysis was performed on a Waters HPLC system consisting of a pump (Model 510, Waters, USA) and UV detector (Model 486 Tunable Absorbance Detector, Waters, USA). The C_{18} reverse phase column (XTerra® 5 μm, 4.6 mm × 150 mm) was used at room temperature. Citrate (33 mM)–phosphate buffer solution (pH 2.0)–methanol-dioxane (36:4:1, v/v/v) was used as mobile phase. The injection volume was 10 μl, and the flow rate was 2.0 ml/min and the signal was monitored at 254 nm.

2.12. Intrinsic dissolution rate (IDR) study

IDR studies were performed by the stationary disc (0.5 cm^2 surface area, Distek Inc., USA) method using the USP XXVIII paddle method using UDT-804 (Logan Instruments Corp. USA). Discs were prepared compressing 100 mg of cefdinir powder in a PerkinElmer hydraulic press for 1 min under 1000 psi. Analysis of the compressed discs by DSC, FT-IR and PXRD confirmed that the crystal form of the original powder was retained following the compression procedure. IDR studies, under sink conditions, were performed in 900 ml of distilled water at 25 ± 0.5 °C and 50 rpm. Suitable aliquots were withdrawn in certain time intervals and filtered using a 0.2 μm nylon syringe filter. At each sampling time, an equal volume of the test medium was replaced. Filtered samples were analyzed for drug concentration by HPLC. Experiment was performed in triplicated.

2.13. Preparation of tablet

Tablet was prepared by mixing D-mannitol, PVP K30, cefdinir and magnesium stearate (weight ratio of 10:30:3:2) using Erweka AR400 (Germany). Homogeneous mixture was directly compressed containing equivalent dose of 60 mg of cefdinir by round punches and dies with a 9 mm diameter. The hardness was controlled at 7 ± 1 kP.

2.14. Dissolution study

Dissolution studies were performed according to the USP XXVIII paddle method using UDT-804 (Logan Instruments Corp. USA). The stirring speed was 50 rpm, and the temperature was maintained at 37 ± 0.5 °C. Each test was carried out in 900 ml of pH 6.8 phosphate buffer. Prepared tablets, containing the equivalent of 60 mg of cefdinir, were placed in the dissolution medium. Then, suitable aliquot sample was withdrawn in certain time intervals and filtered using a 0.2 μm nylon syringe filter. At each sampling time, an equal volume of the test medium was replaced. Filtered samples were appropriately diluted with mobile phase and analyzed for drug concentration by HPLC. Experiment was performed in triplicated.

3. Results and discussion

In this study, amorphous cefdinir particles were obtained from two different processes, SD and SAS-process, respectively. TGA, DSC, PXRD, FT-IR, BET, particle size analysis, pharmaceutically important solid-state properties including solubility, intrinsic dissolution rate and tablet dissolution were studied to characterize the particles obtained by SD- and SAS-process.

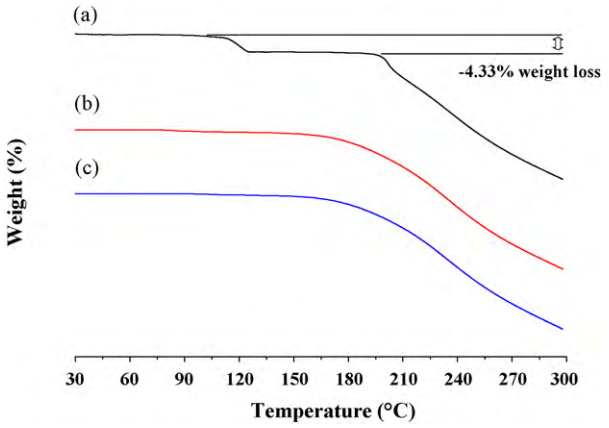

Fig. 2. TGA curves of (a) unprocessed crystalline cefdinir, (b) SD-processed amorphous cefdinir and (c) SAS-processed. amorphous cefdinir.

The TGA curves of unprocessed and all processed cefdinir particles are shown in Fig. 2. The theoretical stoichiometric value of the monohydrate should be 4.35%. The onset temperature and weight loss for unprocessed particles was around 100 °C and about 4.33%, respectively, due to the water loss. The total weight loss corresponding to water loss of about 4.33% is in agreement with stoichiometric value of monohydrate. However, this weight loss was not seen for all processed particles which meant that they existed in anhydrous form. In addition, degradation started at 195 °C for unprocessed particles, while degradation for all processed particles started around 165 °C, which meant that the processed particles were more unstable. From these TGA results, it can be concluded that unprocessed cefdinir were transformed to anhydrous form by SD- and SAS-processes.

Fig. 3 shows the DSC curves of unprocessed and all processed particles. The DSC curves of unprocessed cefdinir, two endotherms at 48.33 and 138.98 °C and exotherm at 195.6 °C were observed; these results were in good agreement with the reported DSC curve of cefdinir monohydrate (Mahendru et al., 2006). The endotherm at 138.98 °C indicated the loss of water and the sharp exotherm at 195.6 °C represented the degradation of the drug as it was shown in TGA results. However, no endotherms were observed in the DSC curves for SD- and SAS-processed particle, which had good agreement with TGA results that the processed particles were anhydrous. The broad exotherm ranging from 160 to 220 °C indicating drug degradation was observed. Since the onset temperature of the degradation was shifted to lower temperature with broadened

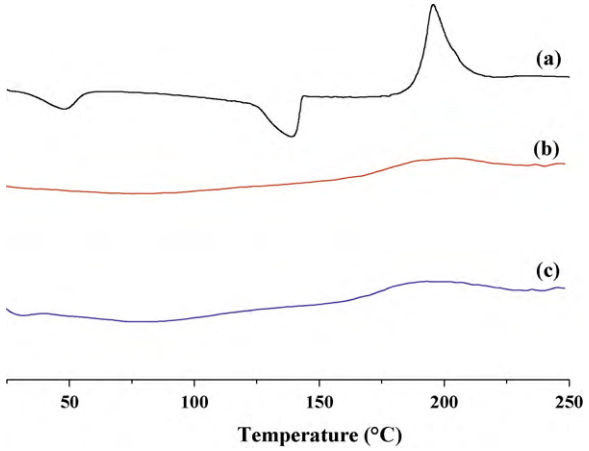

Fig. 3. DSC traces of (a) unprocessed crystalline cefdinir, (b) SD-processed amorphous cefdinir and (c) SAS-processed amorphous cefdinir.

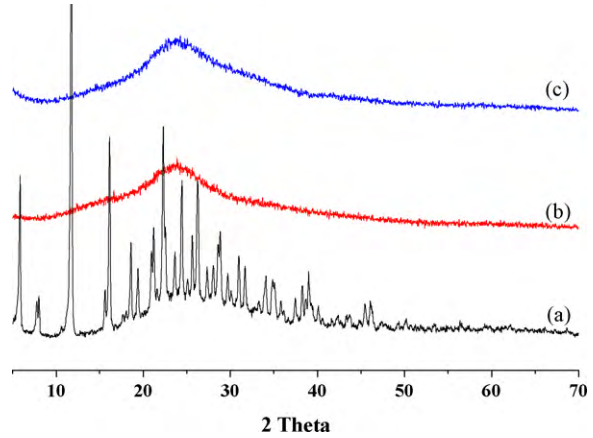

Fig. 4. PXRD patterns of (a) unprocessed crystalline cefdinir, (b) SD-processed amorphous cefdinir and (c) SAS-processed amorphous cefdinir.

peak and endotherms were disappeared, it can be assumed that crystallinity changed to amorphous, which is unstable high energy form (Hancock and Zografi, 1997). These results showed good correlation with TGA results. The PXRD patterns of unprocessed and processed particles are shown in Fig. 4.

The PXRD pattern of unprocessed cefdinir showed characteristic peaks at 5.85°, 7.75°, 11.7°, 16.1°, 21.15°, 22.25°, 24.4°, 26.2° and 28.8° of 2θ (Aleem et al., 2008). On the other hand, all processed particles were characterized by the complete absence of any diffraction peak corresponding to crystalline form of cefdinir. Fig. 5 showed FT-IR spectra of unprocessed and processed cefdinir. The significant differences in the observed vibrational transitions and the bands in the spectrum of the crystalline form were clearer and sharper than the bands of the amorphous forms. In addition, in IR-spectra, it is already known that significant differences between hydrate and anhydrate form were observed around 2800–3800 cm^{-1} (Di Martino et al., 2001). Due to the O–H stretching vibration of water molecules (Cabri et al., 2006), the unprocessed cefdinir, which is in monohydrate form, had characteristic peaks observed at 1133.7, 1188.6, 1666.1, 1781.1, 3296.4, 3596.7 cm^{-1}, but not in processed particles. According to TGA, DSC, PXRD and FT-IR results, they showed good correlation with each other.

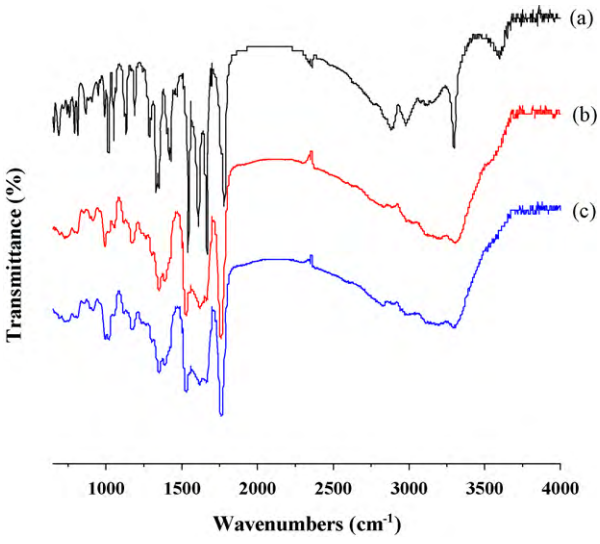

Fig. 5. FT-IR spectra of (a) unprocessed crystalline cefdinir, (b) SD-processed amorphous cefdinir and (c) SAS-processed amorphous cefdinir.

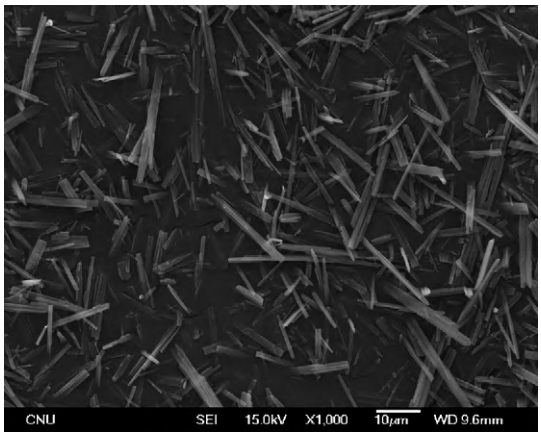

Fig. 6. SEM image of unprocessed crystalline cefdinir particles (×1000).

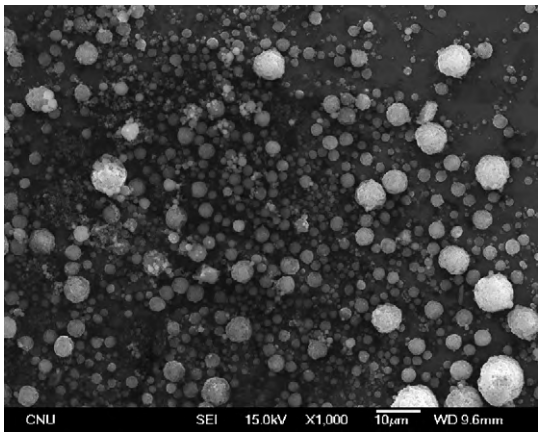

Fig. 7. SEM image of SD-processed amorphous cefdinir particles (×1000).

The SEM images of unprocessed and processed cefdinir are presented in Figs. 6–8. While unprocessed cefdinir particles (Fig. 6) have needle-like crystals, drastic change in the morphology and shape of particles were observed for both processed particles. SD- and SAS-processed particles were observed as spherical agglomerated micro- and nano-particles, respectively. The particle size and specific surface area of unprocessed and all processed particles are summarized in Table 1. The SD- and SAS-processed particles had mean particle size of 2.32 ± 1.76 and 0.15 ± 0.07 μm, respectively.

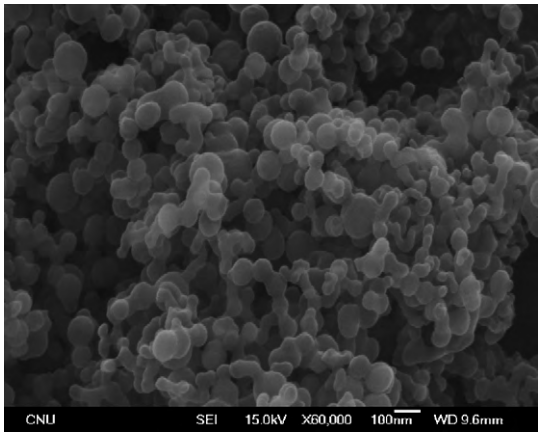

Fig. 8. SEM image of SAS-processed amorphous cefdinir particles (×60,000).

Table 1
Mean particle size and BET of unprocessed and processed cefdinir.

	Unprocessed cefdinir	SD-processed	SAS-processed
Mean particle size (μm)	Needle-like shape with irregular length	2.32 ± 1.76	0.15 ± 0.07
BET surface area (m^2/g)	7.34 ± 0.01	35.01 ± 0.63	55.79 ± 0.06

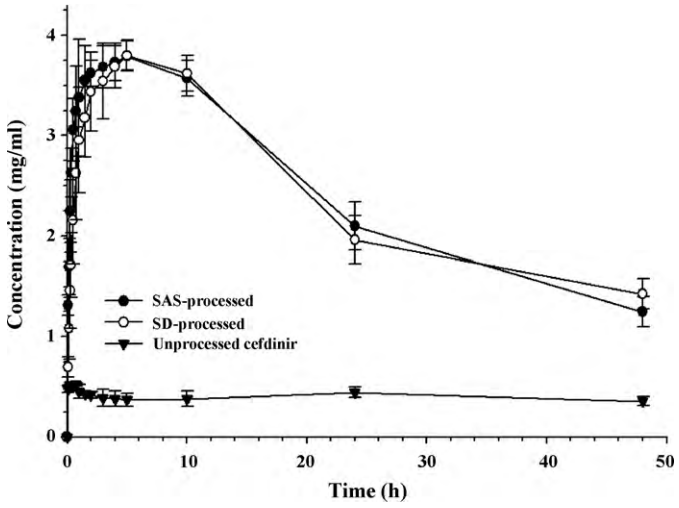

Fig. 9. Kinetic solubility curves of unprocessed cefdinir, SD- and SAS-processed powder.

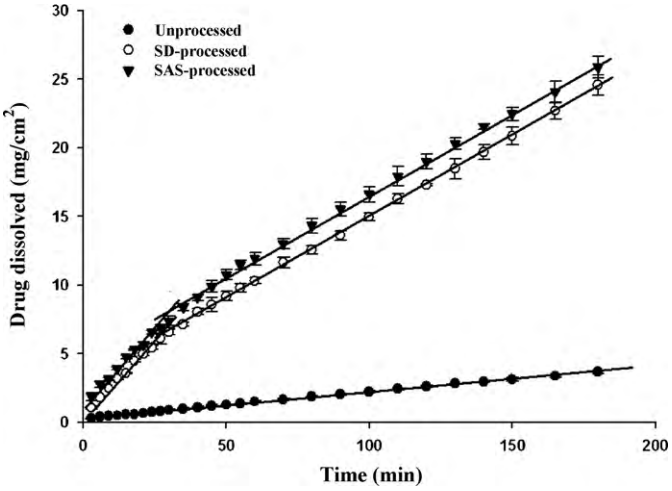

Fig. 10. Intrinsic dissolution profiles of unprocessed, SD- and SAS-processed samples.

The kinetic solubility of all unprocessed and processed cefdinir particles are shown in Fig. 9. In the case of unprocessed cefdinir particle, the equilibrium solubility (approximately 502.1 μg/ml) was reached rapidly. In contrast, the maximum supersaturated cefdinir concentrations for all processed particles, almost similar about 3.8 mg/ml, were not reached immediately, since all the particles were floating on the surface of the water for the several hours until they were all wetted. This is because a micronized particle tends to adsorb air and becomes difficult to disperse into an aqueous medium (Bhattachar et al., 2002; Perrut et al., 2005). However, as soon as the particles were wetted, they dissolved into the water and the concentration of all processed sample reached a higher level, compared to unprocessed particles. It is suggested that these solubility behaviors of all processed particles might be due to their amorphous nature, having higher Gibbs free energy, with the lack of long-range molecular order resulting in rapid dissolution with a higher maximum supersaturated concentration (Hancock and Zografi, 1997; Chawla and Bansal, 2007). In addition, it can be assumed that, since the SAS-processed particle has smaller particle size, it reached the maximum concentration faster than the SD-processed particles. However, the supersaturated concentration of cefdinir decreased gradually to 1.2 mg/ml after 48 h due to solvent-mediated conversion from the amorphous to crystalline form.

Intrinsic dissolution patterns of all unprocessed and processed cefdinir particles are shown in Fig. 10. Good linearities between time and released amount per unit area were found for unprocessed cefdinir particles. However, decreases in the slope were observed after 30 min for all processed particles. This phenomenon might also be due to solvent-mediated conversion form the amorphous to crystalline form.

Under sink conditions, the intrinsic dissolution rate J of a solid is given by:

$$J = kC_s \quad (1)$$

where the mass transfer coefficient is, $k = D/h$, where D is the diffusivity of the solid and h is the thickness of the diffusion layer, which depends on the geometry of the system and of stirring conditions. Since hydrodynamic conditions were controlled to have identical numerical value, the intrinsic dissolution rate constant of unprocessed cefdinir and all processed particles must be equal and the Eq. (1) leads to

$$\frac{J_A}{J_C} = \frac{C_A}{C_C} \quad (2)$$

where J_A and C_A are the mass flux and solubility for amorphous form, respectively, and J_C and C_C are the mass flux and solubility of crystalline form, respectively (Khankari and Grant, 1995). As shown in Fig. 10, unprocessed, SD- and SAS-processed cefdinir were compared. While good linearity was observed between all points for unprocessed cefdinir (the correlation coefficient was 0.9986), a decrease in the slope was observed after around 30 min

Table 2
Intrinsic dissolution rates and solubilities of unprocessed, SD- and SAS-processed cefdinir in water at 37 °C.

	Intrinsic dissolution rate (μg/min/cm^2)		Solubility (μg/ml)	
Unprocessed	19.1		502.1[a]	
	Initial-phase	Second-phase	Estimated solubility	Peak concentration
SD-processed	180.2	106.2	4737.1[b]	3790.[c]
SAS-processed	190.2	116.2	5000.0[b]	3797.3[c]

[a] Observed value.
[b] Estimated solubility.
[c] Observed maximum supersaturated concentration.

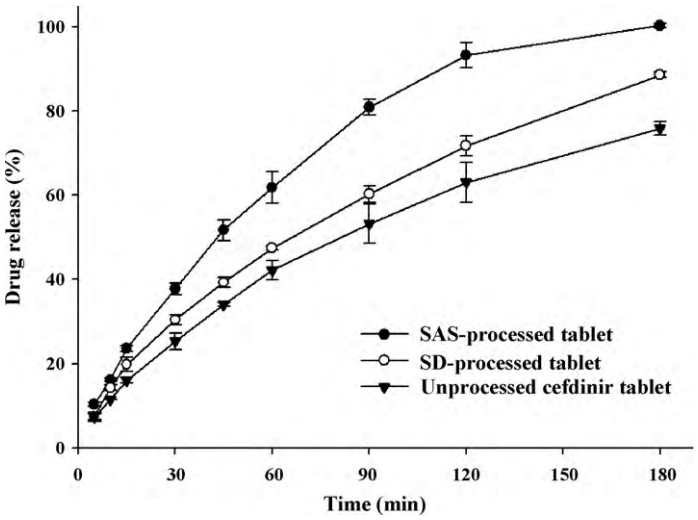

Fig. 11. Drug release profiles of compressed tablet.

for both SD- and SAS-processed cefdinir, which were in amorphous forms. The IDR of SD- and SAS-processed cefdinir at 30 min were calculated and were increased 9.42 and 9.94-fold, respectively, as compared to intrinsic dissolution rate of unprocessed cefdinir (Table 2). The saturated concentrations of SD- and SAS-processed amorphous samples could be estimated from these values. However, the estimated solubility for amorphous samples was slightly different to the observed maximum concentration. Since all of the particles did not make contact with the water immediately, the primarily dissolved particles probably converted to crystalline form before reaching the maximum concentration. Therefore, the observed peak concentrations of SD- and SAS-processed particle were 7.54 and 7.56-fold. As a result of intrinsic dissolution, drug release for the amorphous form (SD and SAS) was always higher than that for the crystalline form (unprocessed), indicating faster drug release.

Fig. 11 shows the dissolution profiles of tabletted samples in a pH 6.8 enzyme free simulated gastric fluid. According to the Noyes–Whitney relationship, the dissolution rate is directly proportional to the particle surface area and the BET results of SAS, SD and unprocessed cefdinir were 55.79 ± 0.06, 35.01 ± 0.63 and 7.34 ± 0.01, respectively. Therefore, enhancement of the in dissolution rate should be clearly observed for SAS- and SD-processed tablet, when compared to the unprocessed cefdinir tablet. Approximately 40% and 30% of the cefdinir was released from SAS-processed and SD-processed tablets after 30 min, respectively, while 25% of unprocessed cefdinir was released in the same time period. Complete drug dissolution was reached after only 180 min for the SAS-processed tablet. In particular, the SAS-processed tablet exhibited faster dissolution than SD-processed tablet. This could be explained by the reduced particle size of SAS-processed particles.

4. Conclusions

In this study, amorphous cefdinir was successfully prepared to have different particle sizes by SD- and SAS-process and their physicochemical properties were evaluated. Through the physicochemical assessment, amorphous cefdinir was in anhydrous form and had a higher apparent solubility compared with unprocessed crystalline cefdinir due to their amorphous nature. In addition, intrinsic dissolution rate showed good correlation with the solubility. By reducing the size of the particles, thereby increasing the specific surface area, the kinetic solubility and dissolution of the SAS-processed sample were faster than the SD-processed sample.

This study demonstrated the usefulness of the micronized amorphous system as a method of enhancing the solubility and dissolution rate of cefdinir. Furthermore, the SAS-process is an efficient tool for improving the dissolute by combining the benefits of an amorphous form and maximizing surface area.

Acknowledgments

This work was supported by the National Research Foundation (NRF) of Korea grant (No. 2008-0060533), funded by (MEST) of the Korean government.

References

Al-Marzouqi, A.H., Shehatta, I., Jobe, B., Dowaidar, A., 2006. Phase solubility and inclusion complex of itraconazole with beta-cyclodextrin using supercritical carbon dioxide. J. Pharmaceut. Sci. 95, 292–304.
Aleem, O., Kuchekar, B., Pore, Y., Late, S., 2008. Effect of [beta]-cyclodextrin and hydroxypropyl [beta]-cyclodextrin complexation on physicochemical properties and antimicrobial activity of cefdinir. J. Pharmaceut. Biomed. Anal. 47, 535–540.
Bhattachar, S.N., Wesley, J.A., Fioritto, A., Martin, P.J., Babu, S.R., 2002. Dissolution testing of a poorly soluble compound using the flow-through cell dissolution apparatus. Int. J. Pharm. 236, 135–143.
Budavari, S., 1996. The Merck Index.
Cabri, W., Ghetti, P., Alpegiani, M., Pozzi, G., Justo-Erbez, A., Perez-Martinez, J.I., Villalón-Rubio, R., Mondero-Perales, C., Munoz-Ruiz, A., 2006. Cefdinir: a comparative study of anhydrous vs. monohydrate form: microstructure and tabletting behaviour. Eur. J. Pharm. Biopharm. 64, 212–221.
Chawla, G., Bansal, A.K., 2007. A comparative assessment of solubility advantage from glassy and crystalline forms of a water-insoluble drug. Eur. J. Pharmaceut. Sci. 32, 45–57.
Chiou, W.L., Reigelman, S., 1971. Pharmaceutical applications of solid dispersion systems. J. Pharmaceut. Sci. 60, 1281–1302.
Dhumal, R.S., Biradar, S.V., Yamamura, S., Paradkar, A.R., York, P., 2008. Preparation of amorphous cefuroxime axetil nanoparticles by sonoprecipitation for enhancement of bioavailability. Eur. J. Pharm. Biopharm. 70, 109–115.
Di Martino, P., Barthélémy, C., Palmieri, G.F., Martelli, S., 2001. Physical characterization of naproxen sodium hydrate and anhydrate forms. Eur. J. Pharmaceut. Sci. 14, 293–300.
Engel, G.L., Farid, N.A., Faul, M.M., Richardson, L.A., Winneroski, L.L., 2000. Salt form selection and characterization of LY333531 mesylate monohydrate. Int. J. Pharm. 198, 239–247.
Ford, J.L., Elliott, P.N.C., 1985. The effect of particle size on some in-vitro and in-vivo properties of indomethacin-polyethylene glycol 6000 solid dispersions. Drug Dev. Ind. Pharm. 11, 537–549.
Han, H.-K., Choi, H.-K., 2007. Improved absorption of meloxicam via salt formation with ethanolamines. Eur. J. Pharm. Biopharm. 65, 99–103.
Hancock, B.C., Parks, M., 2000. What is the true solubility advantage for amorphous pharmaceuticals? Pharm. Res. 17, 397–404.
Hancock, B.C., Zografi, G., 1997. Characteristics and significance of the amorphous state in pharmaceutical systems. J. Pharmaceut. Sci. 86, 1–12.
Jun, S.W., Kim, M.-S., Kim, J.-S., Park, H.J., Lee, S., Woo, J.-S., Hwang, S.-J., 2007. Preparation and characterization of simvastatin/hydroxypropyl-[beta]-cyclodextrin inclusion complex using supercritical antisolvent (SAS) process. Eur. J. Pharm. Biopharm. 66, 413–421.
Khankari, R.K., Grant, D.J.W., 1995. Pharmaceutical hydrates. Thermochim. Acta 248, 61–79.
Kim, E.-J., Chun, M.-K., Jang, J.-S., Lee, I.-H., Lee, K.-R., Choi, H.-K., 2006. Preparation of a solid dispersion of felodipine using a solvent wetting method. Eur. J. Pharm. Biopharm. 64, 200–205.
Kim, J.-S., Kim, M.-S., Park, H.J., Jin, S.-J., Lee, S., Hwang, S.-J., 2008a. Physicochemical properties and oral bioavailability of amorphous atorvastatin hemi-calcium using spray-drying and SAS process. Int. J. Pharm. 359, 211–219.
Kim, M.-S., Jin, S.-J., Kin, J.-S., Park, H.J., Song, H.-S., Neubert, R.H.H., Hwang, S.-J., 2008b. Preparation, characterization and in vivo evaluation of amorphous atorvastatin calcium nanoparticles using supercritical antisolvent (SAS) process. Eur. J. Pharm. Biopharm. 69, 454–465.
Kim, M.-S., Lee, S., Park, J.-S., Woo, J.-S., Hwang, S.-J., 2007. Micronization of cilostazol using supercritical antisolvent (SAS) process: effect of process parameters. Powder Technol. 177, 64–70.
Linpinski, C.A., Lombardo, F., Dominy, B.W., Feeney, P.J., 1997. Experimental and computational approaches to estimate solubility and permeability in drug discovery and development settings. Adv. Drug Deliv. Rev. 23, 3–25.
Mahendru, M., Aryan, R., Chander, Kumar, S., Pandya, B., SanJam, D., Sanjay, G., Yatendra, K., 2006. Crystalline forms of cefdinir. WO/2006/018807, 23 February.

Park, M.-J., Ren, S., Lee, B.-J., 2007. *In vitro* and *in vivo* comparative study of itraconazole bioavailability when formulated in highly soluble self-emulsifying system and in solid dispersion. Biopharm. Drug Dispos. 28, 199–207.

Peeters, J., Neeskens, P., Tollenaere, J.P., Remoortere, P.V., Brewster, M.E., 2002. Characterization of the interaction of 2-hydroxypropyl-beta-cyclodextrin with itraconazole at pH 2, 4, and 7. J. Pharmaceut. Sci. 91, 1414–1422.

Perrut, M., Jung, J., Leboeuf, F., 2005. Enhancement of dissolution rate of poorly-soluble active ingredients by supercritical fluid processes. Part I. Micronization of neat particles. Int. J. Pharm. 288, 3–10.

Perry, C.M.S., Lesley, J., 2004. Cefdinir: a review of its use in the management of mild-to-moderate bacterial infections. Drugs 64, 1433–1464.